Effect of Mg incorporation on the properties of PCL/Mg composites for potential tissue engineering applications

Sumama Nuthana Kalva[1]*, Fawad Ali[1], Kripa Subhadra Keyan[2], Omar M. Khan[2], Mujaheed Pasha[3], Carlos A. Velasquez[4] and Muammer Koç[1]

[1]Division of Sustainable Development, College of Science and Engineering, Hamad Bin Khalifa University, Qatar Foundation, Doha, Qatar, [2]Division of Biological and Biomedical Sciences, College of Health and Life Sciences, Hamad Bin Khalifa University, Qatar Foundation, Doha, Qatar, [3]Core Labs, Hamad Bin Khalifa University, Qatar Foundation, Doha, Qatar, [4]Surgical Research Section, Innovation Unit, Hamad Medical Corporation, Doha, Qatar

Polycaprolactone (PCL) is a biocompatible polymer readily moldable into various shapes and designs. However, its low mechanical strength and slow biodegradation restrict its use in tissue engineering. Magnesium (Mg), a biocompatible metal with excellent osteoconductivity and biodegradability, is a promising choice for tissue engineering applications. This study investigates the influence of Mg incorporation on the properties of PCL/Mg composites, aiming to evaluate their suitability for 3D-printable (3DP) tissue engineering applications. We synthesized a series of PCL/Mg composites with varying Mg concentrations and characterized their mechanical, thermal, and degradation properties. According to microscopic analysis of the composite films, the Mg particles are dispersed consistently throughout all the compositions. The findings demonstrated that adding Mg influenced PCL's mechanical and thermal properties. The mechanical test results showed that the tensile strength of 15% Mg composite filaments improved by around 10% compared to the neat PCL filaments. However, the elastic modulus decreased by around 50% for the same composition. The thermal study revealed a significant reduction in the degradation temperature from above 400°C for pure PCL to around 300°C for PCL/Mg composite having 15% Mg. Additionally, the weight loss during *in vitro* degradation showed that the presence of Mg had significantly increased the degradation rate of composite samples. Also, Mg incorporation influences cell adhesion, with better attachment observed for 10% Mg 3DP samples. Overall, PCL/Mg composites offer a solution to overcome the limitation of low thermo-mechanical properties typically associated with the PCL.

KEYWORDS

magnesium, composite, 3D printing, PCL, filaments

1 Introduction

Tissue engineering has emerged as a groundbreaking field in regenerative medicine, offering innovative solutions to address the limitations of conventional medical treatments for tissue repair and regeneration (Shayesteh Moghaddam et al.,

2016; Razavi and Huang, 2019). Currently, metals and metallic alloys, including titanium, stainless steel, and Cobalt-Chromium alloys, make up the majority of commercially available implants (Muley et al., 2016; Singh et al., 2018; Xiang et al., 2019; Khoo et al., 2020). The ability to fabricate complex structures with tailored properties is a central challenge in tissue engineering, and additive manufacturing techniques have revolutionized the way researchers approach this challenge (Tran et al., 2022).

Among various additive manufacturing techniques like Stereolithography (SLA), Powder bed fusion (PBF), etc. Fused deposition modeling (FDM) is a much simpler technique (Arif et al., 2023). It uses filaments that are melted and deposited layer-by-layer as per the required design. Among the various materials employed in tissue engineering, polycaprolactone (PCL) stands out as a versatile and biocompatible polymer with proven potential for various tissue engineering applications (Malikmammadov et al., 2018). However, to fully realize the potential of PCL, improvements are required to enhance its properties and bioactivity, enabling it to better interact with living tissues and support the regeneration process (Dwivedi et al., 2020). Caproic acid, one of the breakdown byproducts, is either metabolized in the tricarboxylic acid cycle or removed directly through renal secretion. However, due to its lack of essential toughness and slow degradability qualities for bone tissue engineering applications, PCL alone might not be sufficient (Chen et al., 2022; Wang et al., 2022). Magnesium (Mg) is an essential mineral for bone growth and has been shown to have osteoconductive and osteogenic properties, making it an attractive material for bone tissue engineering (Tsakiris et al., 2021; Ali et al., 2022a; Bairagi and Mandal, 2022). Potentially, combining PCL with Mg in a composite material will result in a 3D-printable filament with the mechanical toughness and bone-stimulating qualities of Mg and the biocompatibility and biodegradability of PCL.

The creation of composite materials that can be printed in three dimensions for bone tissue engineering has gained popularity in recent years. Studies conducted *in vitro* have shown that Mg-incorporated composites encourage many bone cells, such as osteoblasts and osteocytes, to adhere to one another, proliferate, and differentiate (Gollwitzer et al., 2005). The composites' biocompatibility, mechanical attributes, and proliferation can all be impacted by their Mg content (Ali et al., 2023). Bakhshi et al. (2023a) incorporated Mg into the polylactic acid (PLA) matrix and found that the addition of Mg improved the mechanical and biological properties of the scaffolds. As detailed in our prior review, numerous traditional techniques have been used to fabricate polymer/Mg composite scaffolds (Ali et al., 2022b). However, no literature was found on any study on the development and analysis of PCL/Mg composite filaments for FDM.

This research article attempts to address this gap by developing PCL/Mg composites that can be extruded into filaments for 3DP. The central hypothesis of this study revolves around the notion that incorporating Mg can augment the biodegradability and mechanical properties of PCL, thereby expanding its potential for tissue engineering. Four PCL + Mg compositions were created, analyzed, extruded into filaments, and then used to print test samples to evaluate the method's efficacy.

2 Material and methods

2.1 Materials

Sigma Aldrich provided PCL pellets with nominal granule sizes of around 3 mm, melting points of about 60°C, and average molecular weights of roughly 80,000 g/mol (Germany). Nanografi Nanotechnology (Turkiye) supplied the Mg alloy powder (WE43), which had an average particle size of 25–50 μm. The density is 1.145 g/cm^3 at 25°C, and the Melt flow Index at 160°C is 2–4 for 5 Kg of the PCL. The PCL solvent, chloroform (boiling point: 59.5°C–60.5°C, density: 1.48 kg/L), was provided by VWR Chemicals, Germany.

2.2 Preparation of PCL/Mg composite films

The solvent evaporation technique was employed to create the composite films. PCL pellets were added to chloroform to develop a concentration of 125 g/L, and then different concentrations of Mg alloy powder (0 wt%, 5 wt%, 10 wt%, and 15 wt%) were added (Table 1). The mixture was then mechanically agitated for 24 h at 400 rpm. After being poured over a metal plate, the solution was dried for 24 h at room temperature before peeling off. The PCL/Mg composites were removed after the chloroform had evaporated for characterization.

2.3 Characterization of composites

A field emission scanning electron microscope (SEM) was utilized to examine the surface morphology of the composite films (FEI Quanta650FEG). The dried samples were cut into appropriate sizes according to the holder's needs, and their surface morphology was examined. A field emission scanning electron microscope operating at a 2 KV accelerating voltage and a 9.0 mm working distance was used to analyze the composite surface's morphology. Energy-dispersive X-ray spectroscopy was also employed to examine the composition of the composite (FEI Quanta650FEG is used for imaging, and Bruker Quantax400 for EDS).

TABLE 1 Composition of PCL/Mg composites used in this study.

Material	Composition (wt%)	
	PCL	Mg (WE43)
0% Mg	100	00
5% Mg	95	05
10% Mg	90	10
15% Mg	85	15

FIGURE 1
Schematic of the fabrication process.
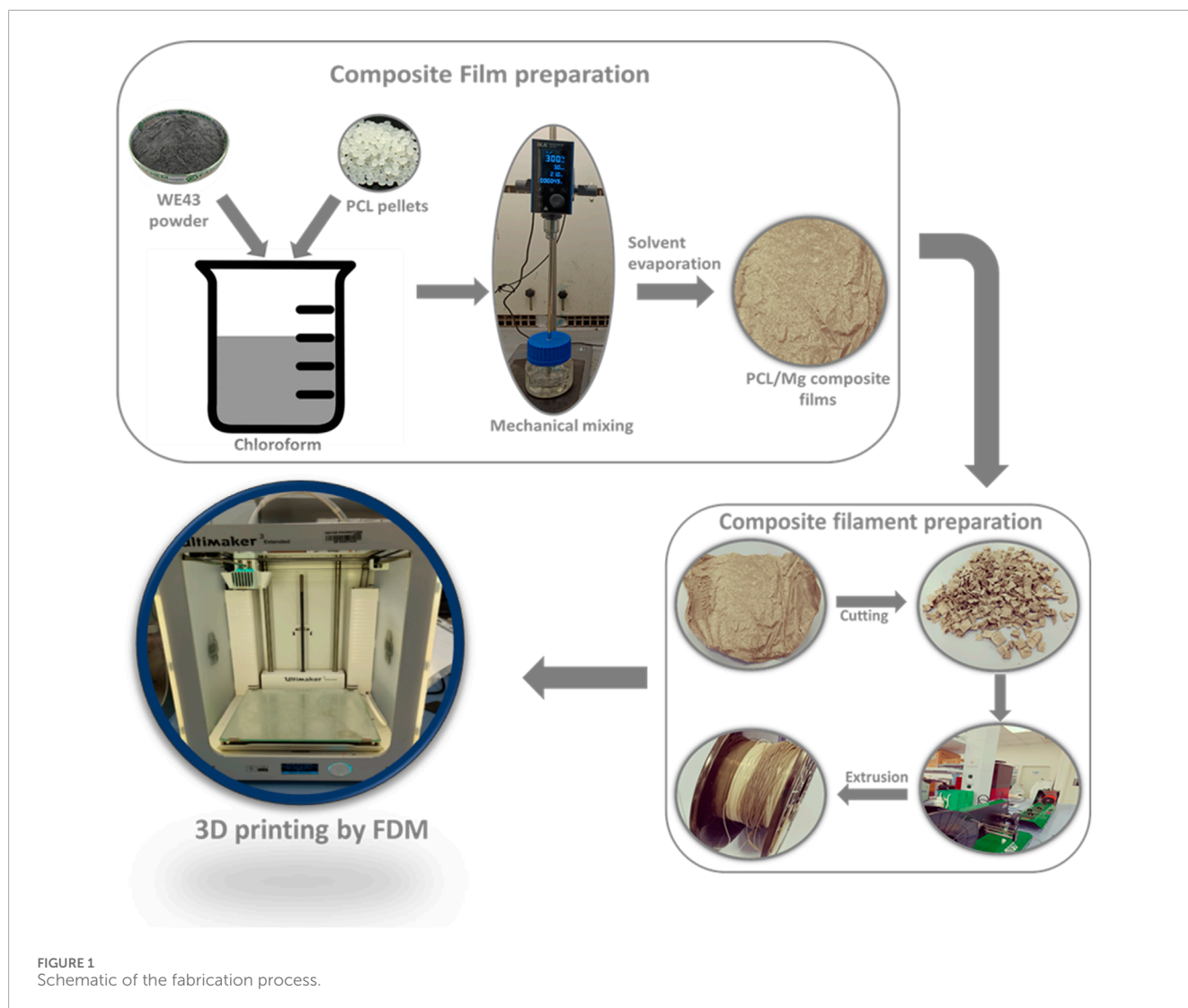
The thermal stability of the PCL/Mg composites was evaluated using the thermogravimetric analysis (TGA) (TA SDT 650). These composites were divided into 10 mg-weight pieces and put into the ceramic crucible. A nitrogen gas purge was used while the heating cycle was configured to heat the material from room temperature to 500°C at 10°C/min. The TGA curves revealed the onset of degradation and the residual mass at 500°C in the composites. The digital scanning calorimetry (DSC) curves revealed the samples' melting point and degradation temperature.

Using Cu K radiation and an angle range of 10°–90° at a scan rate of 0.1°/min, the crystal structures of the composites were identified using the X-ray diffractometer (XRD). The functional groups of PCL/Mg composites were obtained using a Fourier transform infrared spectrometer (FTIR) (FTIR Thermo Scientific Nicolet iS50). FT-IR spectrometer worked in the transmittance mode with an attenuated total reflectance (ATR) sample attachment and a diamond crystal Plate. Spectra in the 4,000–400 cm^{-1} spectrum band at a 4 cm^{-1} spectral resolution were captured using 32 scans per sample.

2.4 PCL/WE43 composite filaments extrusion

The schematic for the sample preparation process used in this paper is shown in Figure 1. For use as feedstock for the extruder, PCL/Mg composites were shredded into uniform-sized squares with a paper cutter. The filament extrusion was done in a Filabot EX2 machine. The filaments were extruded using a 3 mm nozzle diameter at a temperature of 110°C and at a lead screw rotation speed of 20 rpm. Then, these filaments with different Mg concentrations were employed for 3D printing.

2.5 3DP using PCL/WE43 composite filaments

Commercial FDM 3D printers were used to create PCL-Mg samples from the manufactured composite filaments (Ultimaker 3 Extended). The printer's nozzle had a 0.4 mm diameter, while the layer resolution was fixed at 0.2 mm. The 3D printer was fed solid

Cuboid designs with 5 mm × 5 mm × 2 mm dimensions. Solidworks was used to create the scaffolds, and Ultimaker Cura was used to slice the designs for 3D printing. The printer bed temperature was maintained at 40°C, the print speed was held at 20 mm/s, and the printing temperature was set at 160°C. Following a computer-aided design (CAD) file, heated composite filaments were extruded via the 3D printer's nozzle and laid down layer by layer along a specified course. Paper glue was applied to all the materials on the build plate to increase adhesion.

2.6 Mechanical and degradation studies

The composite samples were tested using a MARK-10 testing machine (ESM303, USA). The PCL/Mg composite filaments were put for tensile testing at a uniform pull of 5 mm/min for all the samples. The stress-strain curves were plotted from the load-displacement data obtained from the tests. The values of Young`s modulus and maximum tensile stress data were also extracted from the stress-strain curves. Three scaffolds were mechanically tested for each sample.

The printed samples were weighed and immersed in glass test tubes filled with 10 mL of PBS (phosphate-buffered saline) solution for the degradation experiment. Fourier transform infrared spectrometer (FTIR) was used to detect the functional groups in PCL/Mg composites before and after degradation in PBS solution. By submerging the PCL/Mg scaffolds in PBS solution with an initial pH value of 7.6 for 4 weeks, the degradation of the 3D-printed scaffolds was examined. Before immersion in PBS, the weights of the scaffold were all measured. The weight reduction was calculated after removing the samples from PBS and drying them in an oven at 40°C for 8 h after 2 and 4 weeks. The following calculations were used to calculate the weight loss percentage (W%) of the scaffold:

$$\Delta W\% = \left(W_i - W_f\right)/W_i \times 100\%$$

where W_i and W_f are the initial and final weights of the dried degraded scaffolds, respectively.

The pH change in the media was measured using a PCE Instruments (Spain) PCE 228 pH meter after 4 weeks in PBS.

2.7 Cell culture studies

An *in vitro* cell culture was performed to investigate how the epithelial cell line MCF7 behaved on PCL/Mg scaffolds. Given their origin and primary usage in breast cancer research, using MCF-7 cells—which are generated from human breast adenocarcinoma—for bone tissue engineering applications may not be the most straightforward or obvious decision. Nonetheless, MCF-7 cells can be employed in general biocompatibility analyses to assess the interactions of novel materials with human cells. Despite not being bone cells, their reaction can reveal important details regarding the cytotoxicity or cellular effects of the tested materials.

Cell line MCF-7 was obtained from cell services at the Francis Crick Institute and maintained in RPMI 1640 media (Gibco) supplemented with 10% fetal bovine serum (FBS), 1% glutamax, 1% penicillin/streptomycin (Gibco) and 0.1% Normocin (Invitrogen).

The cell line was maintained in a standard cell culture humidified incubator at 37°C and 5% CO_2.

The scaffolds were treated with ethanol and allowed to air dry, and after 20 min of UV sterilization on each side, they were ready for cell seeding. After sterilization, the samples were rinsed with PBS, soaked in culture media overnight, and then seeded with MCF7 cells at a density of 3×10^4 cells per sample. The purpose of this seeding procedure was to investigate cell attachment.

Scanning electron microscopy (SEM) was used to examine cell attachment on the surfaces of PCL/Mg scaffolds. The cells were fixed with a 4% formaldehyde solution prepared in PBS (Invitrogen FB002) after 48 h and then rinsed in distilled water. The cells were then dehydrated by exposing them to a series of ethanol solutions that increased in concentration (from 50% to 100% [v/v]). The prepared samples were coated with a layer of carbon using sputter coating, and the Philips XL30 model of SEM was used to observe them.
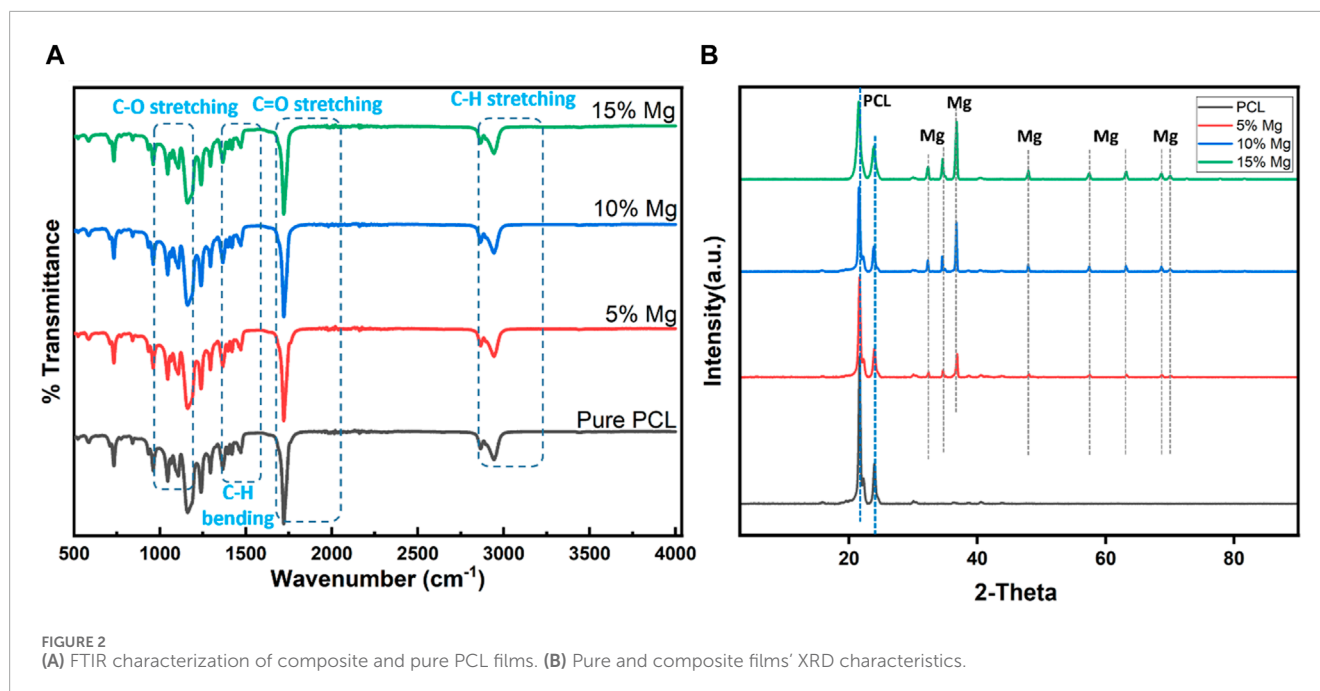
2.8 Statistical analysis

The reliability of the provided results was verified three times for all experimental data and 3D printing results. Results are recorded as mean value ±SD whenever applicable.

3 Results and discussions

3.1 FTIR & XRD results

An FTIR study of the PCL/Mg composite films was carried out to understand the changes in the composite samples' functional groups by adding Mg to the PCL matrix. The FTIR spectra of the PCL/Mg composite materials are shown in Figure 2A, where the absorption bands related to the functional groups found in the PCL matrix can be seen. The little differences between PCL and PCL-Mg composites show that the chemical relationships were similar and consistent with the literature (Antoniac et al., 2019). The spectra reveal the various characteristic peaks associated with the PCL in the composites. There are bands between 2,900 and 3,000 cm^{-1}, which can be attributed to the symmetrical and asymmetric stretching vibrations of the CH group. At around 1,748 cm^{-1}, bands brought on by the stretching vibration of the C=O group begin to appear. Furthermore, it can be concluded that no additional absorption peaks or shifting of peak positions can be observed in the composite samples. This shows that the Mg particles and the polymer matrix mix nicely. The PCL and the Mg particles did not appear to interact chemically during the blending process.

Figure 2B displays the XRD spectra of the PCL and Mg-incorporated samples. The Mg alloy's 2Θ = 32°, 34°, and 36° peaks grew more distinct as the Mg content in the PCL samples rose. The peaks at 2 Θ = 21° and 25°, which correspond to the "α" crystallization phase, show that the pure PCL had a semi-crystalline structure. It is critical to remember that the XRD peaks, which only indicate the crystallinity of a thin surface layer, may not accurately reflect the crystallinity of the bulk material. These findings are consistent with research previously reported in the literature (Hasanpur et al., 2021).

FIGURE 2
(A) FTIR characterization of composite and pure PCL films. **(B)** Pure and composite films' XRD characteristics.

3.2 SEM study of films

SEM study was carried out on the PCL/Mg composite films prepared after the solvent evaporation. This was done to understand the morphology of the produced films. This understanding will help us predict the cell attachment and proliferation behavior as the surface morphology greatly influences them. The SEM images also give an insight into how the Mg particles are distributed across the polymer matrix. Figure 3A shows the PCL matrix's SEM pictures of various WE43 percentages. All the images show the presence of the Mg particles across the surface. This suggests that the mechanical mixing has effectively distributed the particles in the polymer solution. The observed non-uniform dispersion of Mg-based particles within the PCL matrix can be seen as a potential sampling issue. However, the observed non-aggregation of Mg particles will make it easier for extrusion into homogenous filaments for 3DP by potentially avoiding clogging. The topography images of the investigated films show rough surfaces, and incorporating a larger Mg content due to Mg on the surface makes the surface rougher.
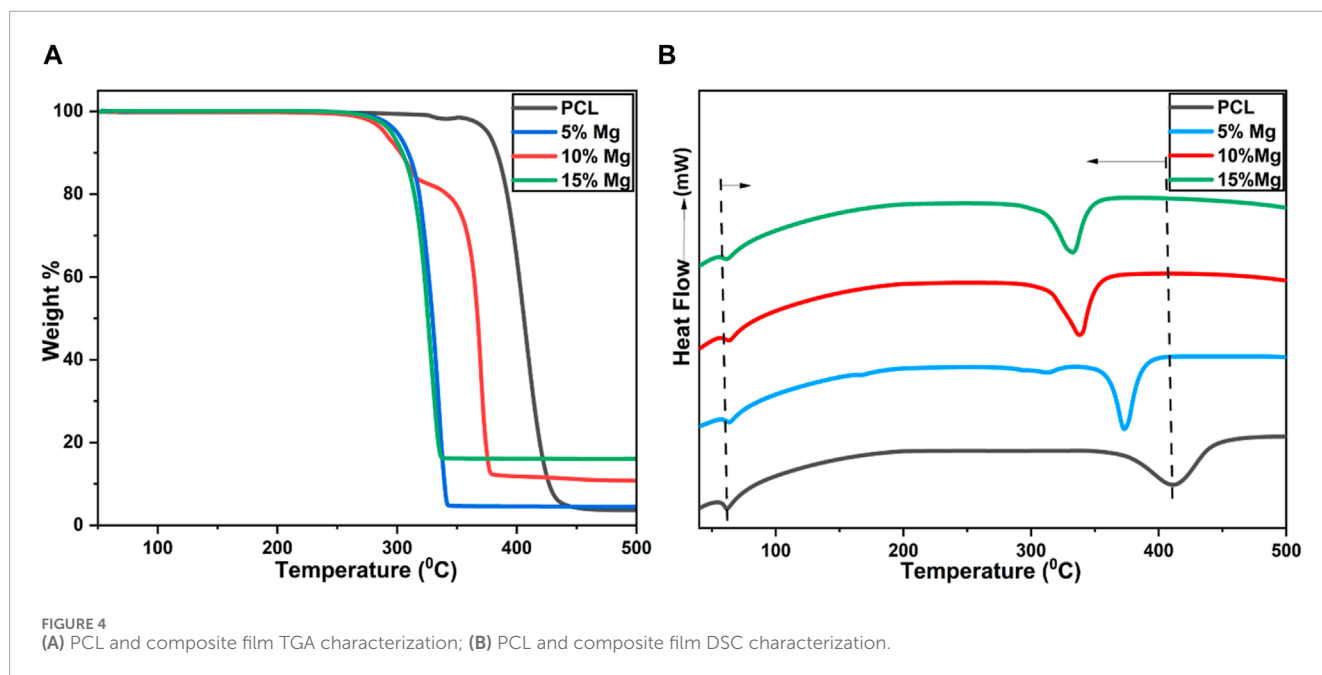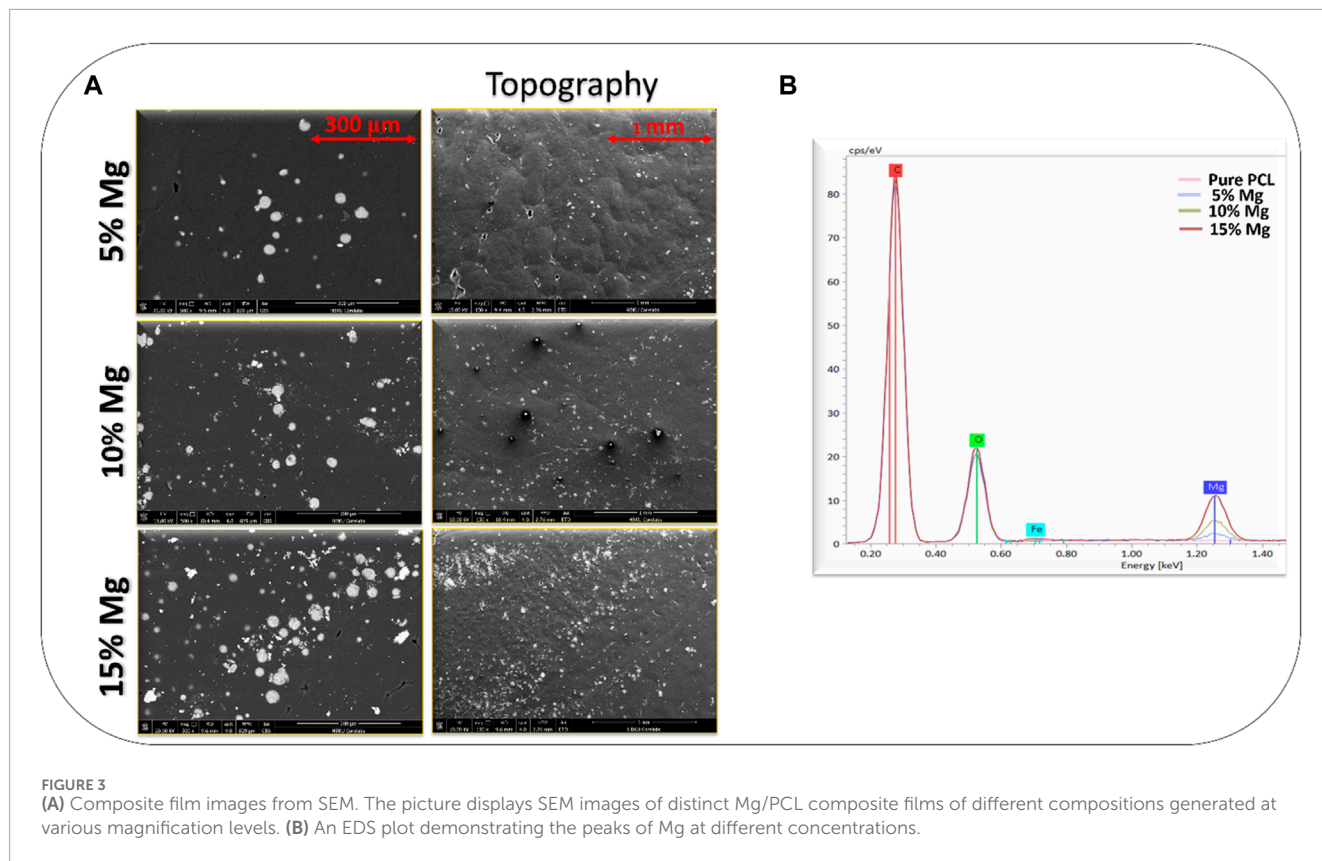
The EDS mapping images of the different PCL/WE43 mixes are shown in Figure 3B. The amount of Mg particles that can be seen on the surface likewise increases when WE43 concentrations rise. As WE43 concentration rises, the peak of Mg particles also rises. This shows that impurities were not incorporated on the surface during the blending process.

3.3 Crystallization and thermal degradation behavior

TGA measurements were made to better understand how the processed materials thermally degraded and investigate the extrusion and printing temperature limitations. Up to about 300°C,

all samples remained largely stable without experiencing any significant weight loss, although PCL was stable even up to about 400°C, corresponding to PCL's breakdown. Thermal degradation of PCL occurs between 380°C and 450°C, whereas thermal degradation of PCL/Mg composites occurs between 280°C and 300°C. This shows that the Mg addition expedites the PCL's heat breakdown. The composite mixtures also displayed a residue quantity, unlike pure PCL, which was completely degraded. This is reasonable given that the residue's remaining component, Mg, may be linked to it. Figure 4A composite samples show that the residual Mg amount values resemble the initial Mg weight percentage. These findings indicate that Mg inclusion accelerates PCL breakdown at high temperatures. When the polymer is heated, Mg behaves as a catalyst for the PCL depolymerization reaction. The literature describes similar thermal analysis results for PLA/Mg composites (Leonés et al., 2023).

DSC thermograms, displayed in Figure 4B, were used to analyze the thermal characteristics of PCL and PCL/Mg scaffolds. With the addition of Mg, the endothermic melting enthalpies also dropped. All samples exhibit two thermal transitions, regardless of the presence of Mg particles. With a melting peak (Tm) at 57°C, the first temperature-related transition is an endothermic phase. When samples contain 15% Mg, the Tm peak peaks at 61°C and climbs with increasing Mg content. All the samples can be compared and examined for PCL properties, such as melting and decomposition temperatures. These findings imply that Mg particles do not significantly affect the PCL melting peaks. Mg particles act as nucleation agents, however, and this causes heterogeneous nucleation in the samples. We obtained comparable results when our research team used the same WE43 particles in the PLA matrix (Kalva et al., 2023). This is essential to remember when developing materials for biomedical applications since changes in chemical composition may have adverse impacts on the body, such as powerful immunological reactions.

FIGURE 3
(A) Composite film images from SEM. The picture displays SEM images of distinct Mg/PCL composite films of different compositions generated at various magnification levels. **(B)** An EDS plot demonstrating the peaks of Mg at different concentrations.

FIGURE 4
(A) PCL and composite film TGA characterization; **(B)** PCL and composite film DSC characterization.

3.4 Characterization of the extruded filaments

PCL/Mg filaments with 0, 5, 10, and 15 wt% Mg were successfully extruded using the filabot extruder (EX2). Melts were extruded from the extruder for each PCL-Mg composition over a period of time while being watched in real time to ascertain when the desired filament diameter of d = 2.75 ± 0.25 mm was obtained. The Ultimaker 3 Extended printer can only be used with filaments that fall within this range in diameter. It was observed that the even though the melting temperature was around 60°C, proper extrusion of the filaments was feasible only at 110°C. This could be associated
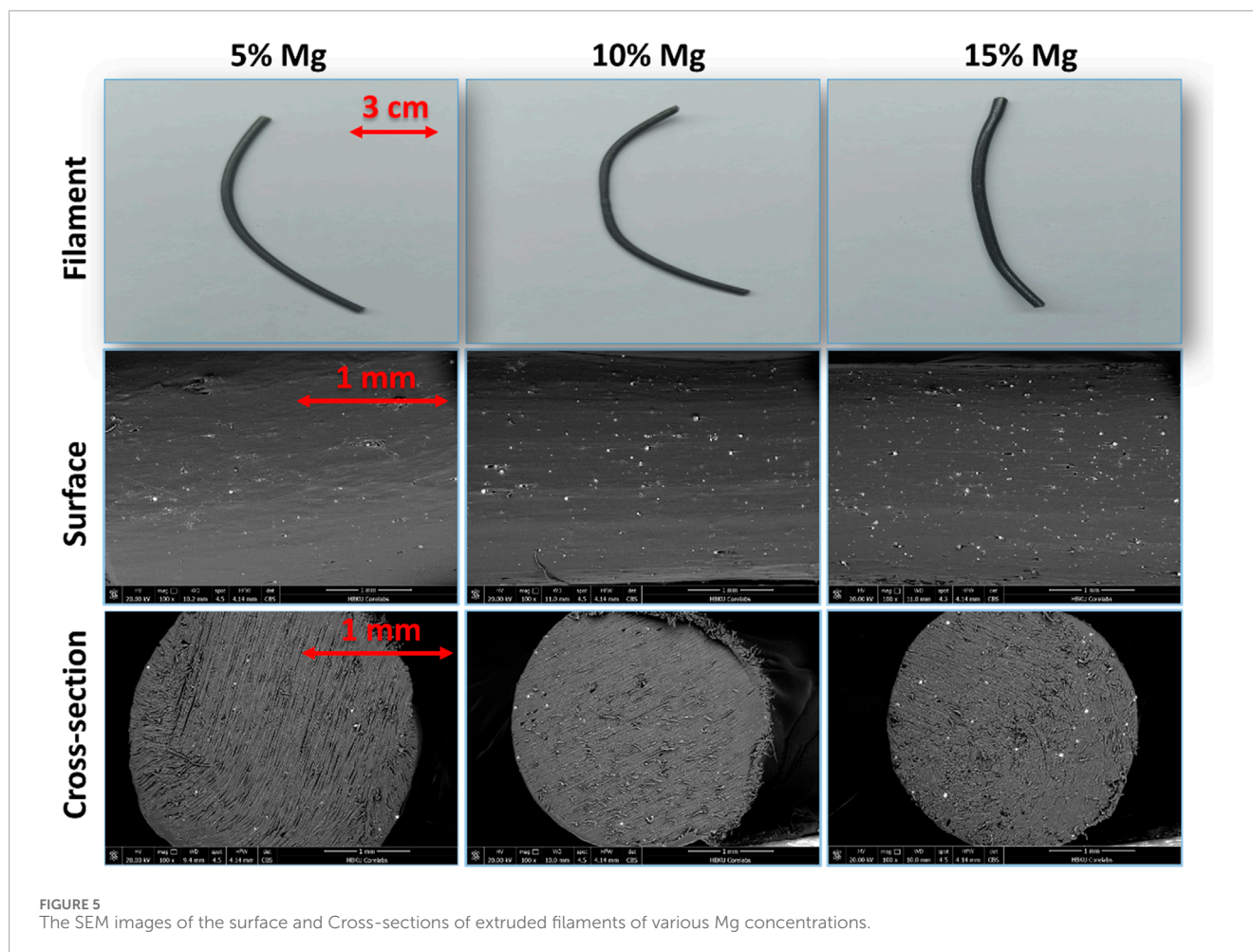
FIGURE 5
The SEM images of the surface and Cross-sections of extruded filaments of various Mg concentrations.
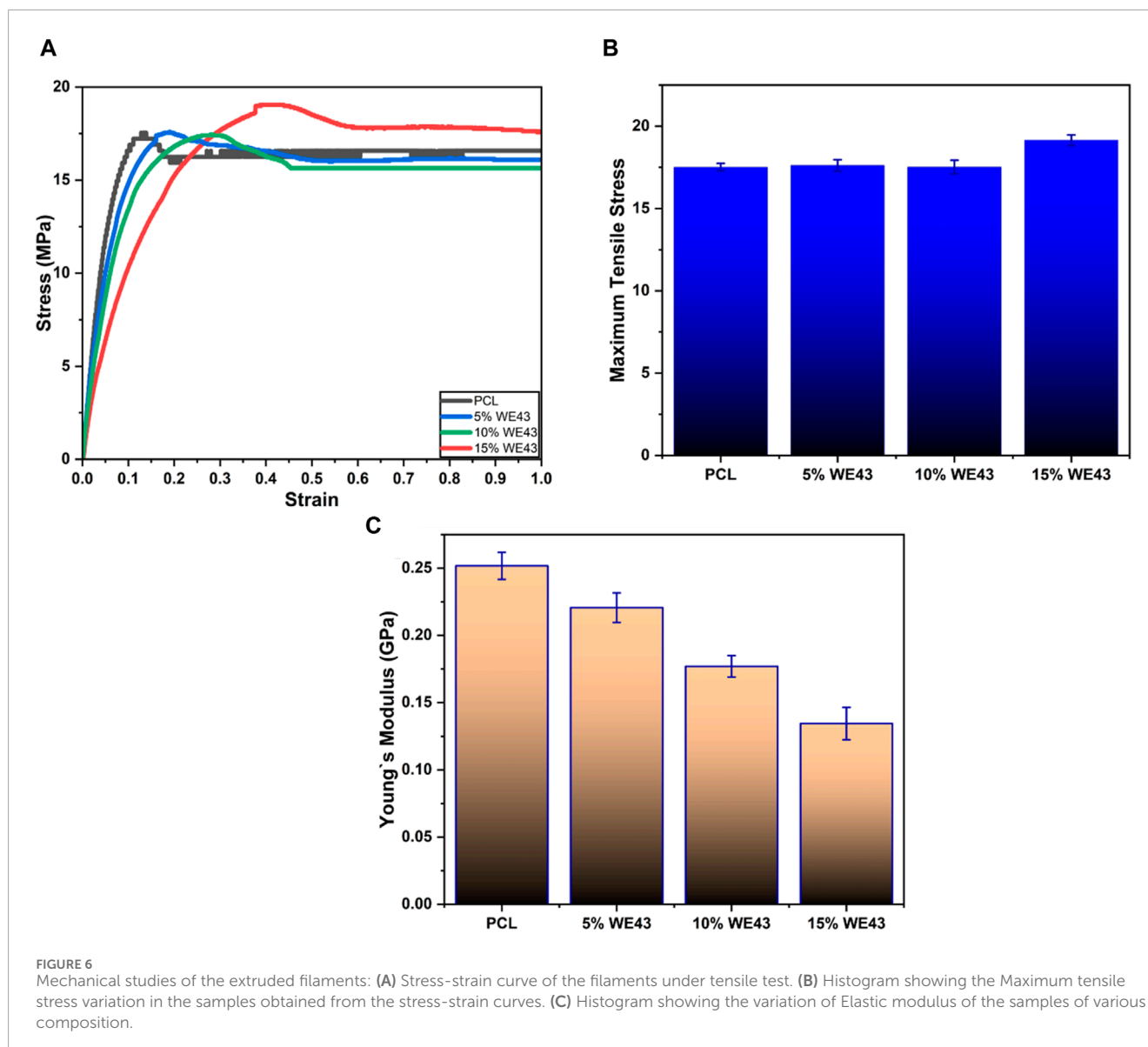
with the better melt flowability of PCL only at higher temperatures. Even though the PCL starts melting at 60°C, factors like high molecular weight and long chains increase entanglement and intermolecular interactions, making it challenging for the material to flow freely. Scanning electron microscopy images demonstrated the homogeneous distribution of the Mg particles within PCL-Mg filaments (Figure 5). The surface of the filaments under investigation is already rough, and the addition of Mg makes it noticeably rougher, as discussed in the earlier discussion on films. As observed in this image, the Mg particles are comparably homogenous and well distributed throughout the PCL matrix, suggesting the mixing and extrusion technique may be useful for creating high-quality PCL/Mg composite filaments.

3.5 Mechanical & degradation studies

Tensile tests were used to assess the mechanical characteristics of PCL and PCL-Mg composite filaments. Figure 6A depicts representative tensile stress-strain curves for PCL-Mg composites with varied Mg contents. These findings show that adding Mg particles to the PCL matrix boosts the tensile strength of PCL samples with a 15% Mg loading. However, when compared to PCL samples, there is no discernible difference in the final tensile strength of the 5% and 10% Mg-loaded samples (Figure 6B). For instance,

adding 15% Mg increases the ultimate tensile strength of plain PCL by 10%. Though this increase is statistically significant, the increase is not practically significant for bone tissue engineering applications. It still falls short of the strength of natural bone, which typically ranges from approximately 50–150 MPa (Noroozi et al., 2023). However, it might still be practically significant if the material serves a purpose where maximal strength is not the primary requirement. The fact that the elongation at break is seen to be greater than 100% strain shows that the composite samples still retain the clean PCL's ductility. The composites produced necking, and the elongation at break is significantly more than the 100% strain threshold. This shows that, in these experimental settings, the Mg powder had no significant effect on the composites' tensile ductility. With increased Mg content in the samples, the elastic moduli of the composites showed a trend toward reduction. This can be seen in Figure 6C. It is discovered that when the Mg weight proportion increases, the elastic modulus of the composites drops linearly. In other words, the stiffness of the PCL/Mg composites is not improved by the Mg addition. It is commonly accepted that the compatibility and interfacial adhesion strength between the components, the strength of the components as well as crystallization in the blends, etc. are directly related to the reinforcement processes for polymer blends (Liang et al., 2013). One of the main processes for reinforcing inorganic particulate-filled polymer composites works as a result of the inorganic particles restricting the movement of the matrix's

FIGURE 6
Mechanical studies of the extruded filaments: **(A)** Stress-strain curve of the filaments under tensile test. **(B)** Histogram showing the Maximum tensile stress variation in the samples obtained from the stress-strain curves. **(C)** Histogram showing the variation of Elastic modulus of the samples of various composition.

macromolecular chains to increase stiffness and strength. The modulus of the reinforcement and the effective crystallization in the blends are the two key factors that affect the stiffness of a polymer composite. As the content of inorganic reinforcements increases, the tensile elastic modulus for composites will drop. For the purpose of estimating particulate-filled systems' Young's moduli, theoretical models have been created. Einstein has determined the simplest model equation for spherical particles inserted in a polymeric phase. According to the volume ratio of particles, a linear relationship between Young's modulus of the composite and Young's modulus of the polymer can be highlighted under specific hypotheses. This model supports the outcomes shown in Figures 6A, C.

Scaffold degradation is influenced by several variables, including the composite's microstructure, porosity, and hydrophilicity. Due to PCL's slower rate of breakdown (1–2 years), which is the lowest of all known biodegradable polymers, PCL may be a better option for open fractures (Arif et al., 2022). Degradation studies were conducted *in vitro* using a PBS solution to determine how PCL's Mg content affects composites' degradation. After being submerged in

PBS for 4 weeks, the PCL and PCL/Mg composites were analyzed using FTIR. To further understand the weight loss of the scaffolds and their durability in a physiological context, their weight loss was carefully monitored after being submerged in PBS for 2 and 4 weeks. As seen in Figure 7A, the degradation rate of PCL/Mg composites has increased as Mg content has increased. The bone scaffold may still be able to maintain developing cells for a longer amount of time to generate more thick tissue because of the comparatively slow disintegration rate (maximum 5.5% at day 28). All the samples showed weight loss, however, there were distinct variations between them. Notably, the PCL scaffolds showed modest changes after 4 weeks and the smallest weight loss at any time. In contrast, the PCL/Mg scaffolds lost weight substantially more than the PCL scaffolds did, and this weight loss increased proportionally with the addition of Mg (Shuai et al., 2018). These findings strongly suggested that the presence of Mg sped up the scaffolds' breakdown process. Weight loss demonstrated the PCL/Mg scaffolds' ability to deteriorate or dissolve and may be replaced by fresh tissue during the tissue regeneration process.
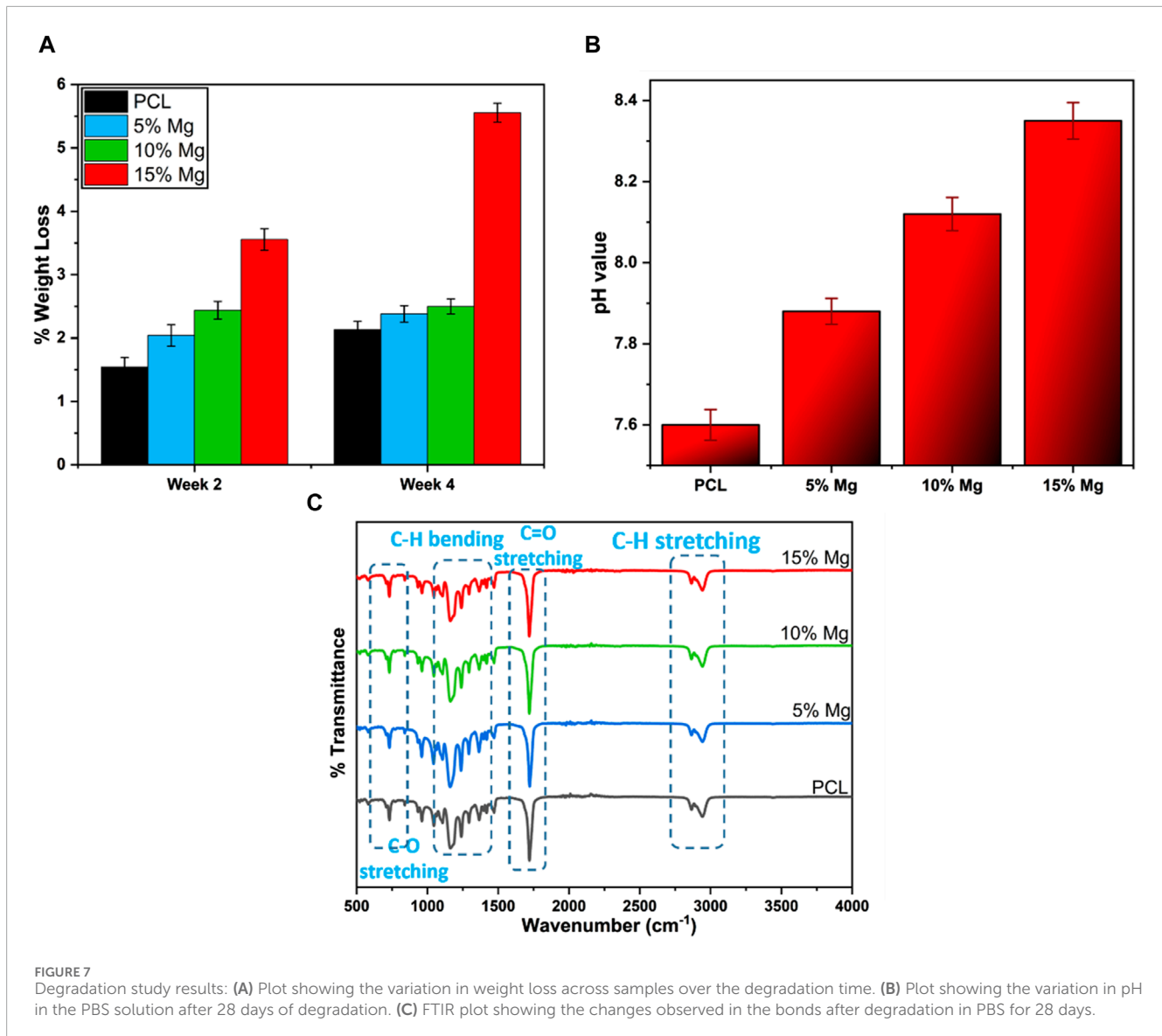
FIGURE 7
Degradation study results: **(A)** Plot showing the variation in weight loss across samples over the degradation time. **(B)** Plot showing the variation in pH in the PBS solution after 28 days of degradation. **(C)** FTIR plot showing the changes observed in the bonds after degradation in PBS for 28 days.

In addition to degradation, the pH value change was measured after 4 weeks of degradation in PBS solution (Figure 7B). The pH values are shown in Figure 7B. The results showed that the pH values of the immersion media displayed a trend toward increasing alkalinity as the concentration of Mg rose in the scaffolds. The pH values increased from 7.6 for pure PCL to 8.35 for the PCL/Mg scaffold containing 15% Mg. This shows that the environment's pH rose due to the degradation of PCL/Mg scaffolds. This alkalinizing effect may have been caused by the release of Mg ions during the breakdown process and the creation of $Mg(OH)_2$ (Song and Atrens, 1999; Shuai et al., 2018). An alkaline environment can affect cell behavior, including proliferation and differentiation. Therefore, the pH stability of degradable scaffolds is an important factor in their design and application. In some cases, a mild increase in pH could be beneficial. For example, a slightly alkaline pH might help with bone tissue engineering, as it can promote the deposition of calcium phosphate minerals, aiding bone regeneration (Galow et al., 2017).

The samples were measured using FTIR to compare and analyze the degradation by immersion in PBS. The FTIR spectra of printed samples containing 5, 10, and 15 wt% of Mg particles in PCL are shown in Figure 7C. Peaks are generally decreasing, and the FTIR graphs show significant noise. This indicates that the bonds corresponding to the different groups in the polymer composites were degrading and gradually disappearing from the samples. Following 4 weeks of immersion in PBS, the peak at 3,000 cm^{-1}, associated with the stretching of the OH group brought on by PCL hydrolysis, exhibits a comparable decline for the sample containing 10 and 15 wt% Mg. When compared to data from non-deteriorated samples, the intensity of the PCL band at 1,747 cm^{-1}, which is related to the carboxyl band and ester group, is much lower for the degraded scaffolds. When a polymer degrades or interacts with another component, the PCL band at 1,747 cm^{-1} becomes very sensitive to these changes, which can result in a decrease in intensity or a downward shift in wavelength. The peak intensity for the samples after week 4 drastically dropped

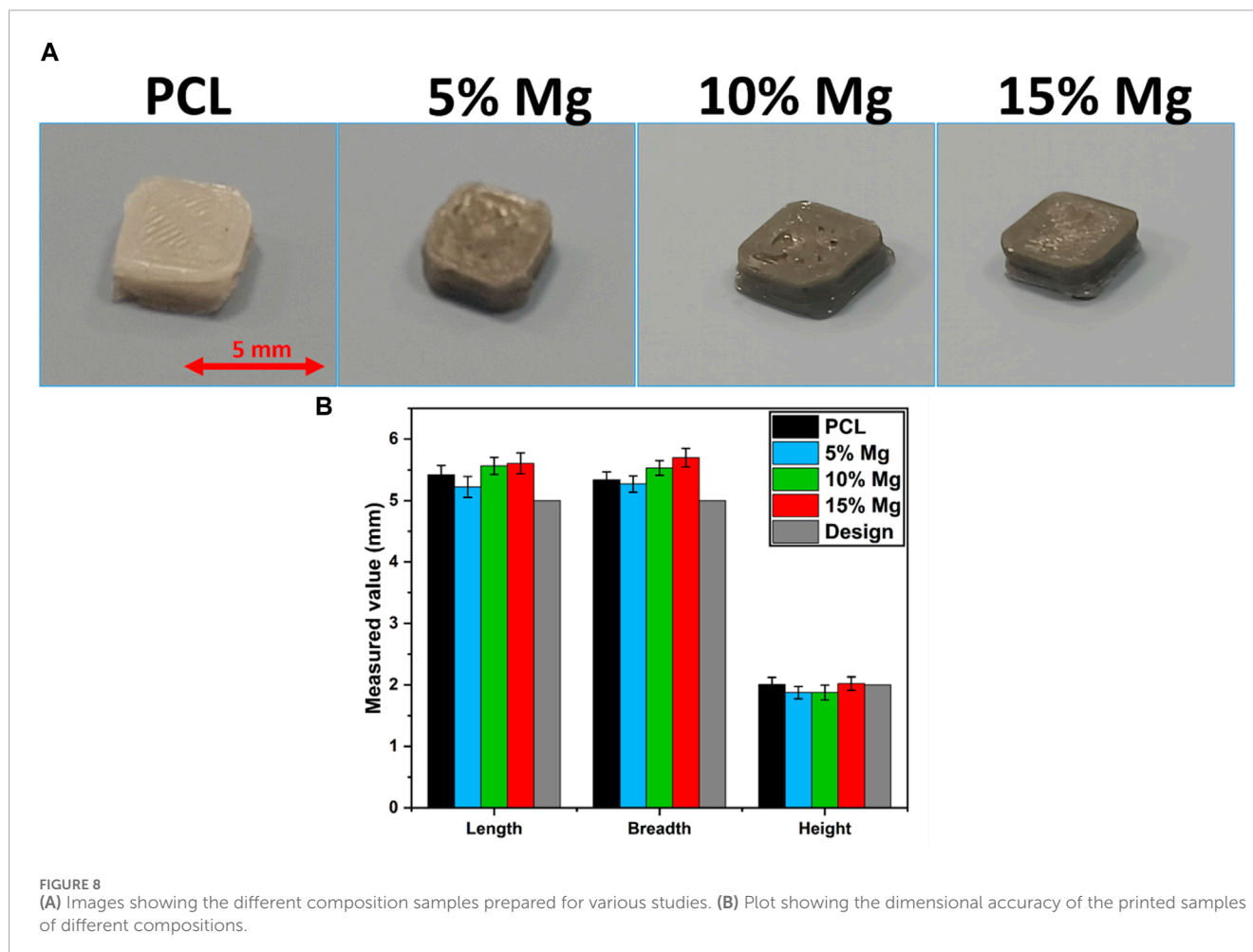TABLE 2 Table displaying all of the FDM printing parameters that are utilized.

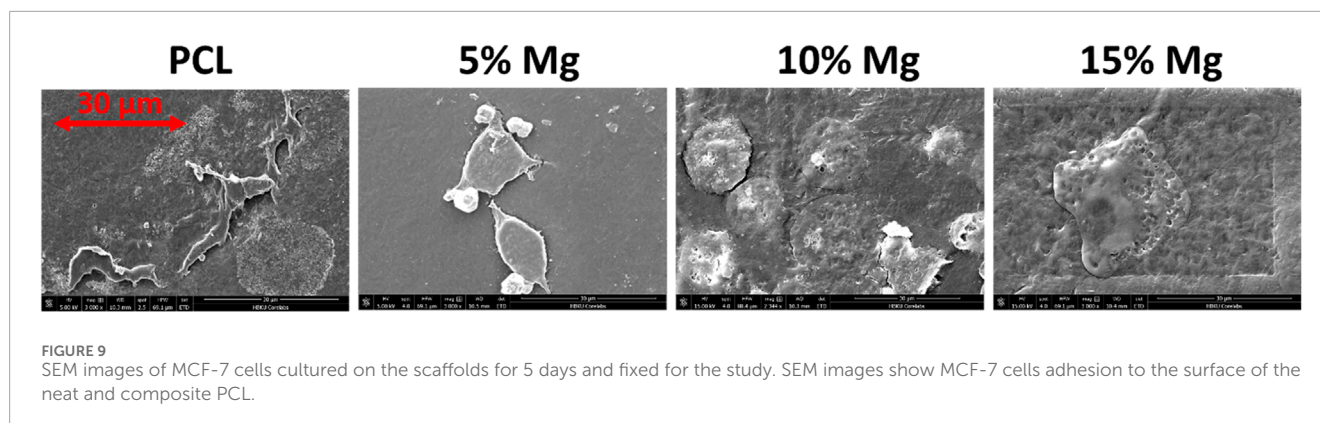| Printing parameters	
Nozzle temp	160°C
Print speed	20 mm/s
Print bed temp	40°C
Layer thickness	0.2 mm
Nozzle dia	0.4 mm

as the Mg concentration rose (Akindoyo et al., 2017; Ferrández-Montero et al., 2020). This indicates the interaction between the ester group (R-COOR') from PCL with Mg particles, resulting in faster PCL/Mg samples degradation.

3.6 3DP of PCL/Mg composite samples

For the FDM technique to properly 3D print PCL/Mg composites, the molten material must flow through the nozzle without clogging at the nozzle tip. To assess the suitability of the prepared composite filaments and their feasibility to be fabricated into complex geometries, all the PCL-Mg composite filaments were 3D printed. According to earlier research, the nozzle temperature for PCL FDM printing must be maintained at 160°C (Tzeng et al., 2018; Cheng et al., 2021). As a result, it was decided to print all compositions at this temperature. The printing process used a 20 mm/s printing speed while keeping the bed temperature at 40°C and the nozzle temperature at 160°C. Table 2 provides a summary of all the printing settings. All composite filaments were discovered to be easily printable and free of any flaws or irregularities. Figure 8A illustrates how the printed components adhered to the input design specifications without materially deviating from the original CAD file. Without any gaps in the layers, the finish was also smooth. This can be explained by the fact that the filaments in the SEM cross-section pictures reported in the previous section did not exhibit pore development. It can be observed in Figure 8B that the dimensional accuracy of the printed samples was close to that of the input design numbers. There was a slight change in the length and breadth of the printed samples for the 5% Mg samples, but the deviation was a bit more prominent in the other samples. This can be attributed to the melts not retaining their shape after deposition on the build plate, leading to spreading after deposition. This might have caused the deviation from the input values. On the other hand, the height

FIGURE 8
(A) Images showing the different composition samples prepared for various studies. (B) Plot showing the dimensional accuracy of the printed samples of different compositions.

FIGURE 9
SEM images of MCF-7 cells cultured on the scaffolds for 5 days and fixed for the study. SEM images show MCF-7 cells adhesion to the surface of the neat and composite PCL.

deviation was observed to be less significant. Based on the data, it can be concluded that the 5% Mg filaments resulted in better 3DP samples as they show much lesser deviation in all directions.

3.7 Cell culture studies

To investigate the cell adhesion on PCL and PCL/Mg composites with 5, 10, and 15% Mg, MCF-7 cells seeded on PCL and PCL/Mg composites after 5 days of culture are presented by FE-SEM images in Figure 9. SEM analysis revealed that the four groups of 3D-printed scaffolds served as an excellent surface for the attachment and proliferation of MCF-7 cells. Cell attachment is a critical aspect to consider in tissue engineering and regenerative applications. In the images, one would typically look for indications of these differences by examining the number of cells attached, the degree to which the cells have spread and flattened out on the surface, and the presence of cellular extensions. These features are indicative of good cell-material interactions, which are critical for tissue engineering applications. Various factors contribute to the cell's adhesion on the scaffold surface, including surface roughness and hydrophilicity (Asadollahi et al., 2022). Mg incorporation into PCL enhances the surface hydrophilicity (Bakhshi et al., 2023b), so the high number of cell attachments to the scaffolds with 10% Mg as compared to pure PCL might be because of the increased hydrophilicity, as reported by Dong et al. (2021). Though all the groups show cell attachment and growth indicating positive cell-material interactions, further quantitative assays need to be done to draw a definite comparison on the influence of Mg on their proliferation over the PCL/Mg scaffolds.

4 Conclusion

This study investigates the development of Mg-filled PCL composites as a potential new material for biomedical applications using 3DP. It presents the viability of these PCL/Mg composites for extrusion into filament form and fabrication into test samples using FDM-based 3DP. The influence of Mg inclusion on PCL's thermal, physicochemical, and printability behavior is evaluated and summarized below:

- The composite films' SEM examination reveals that the Mg particles are evenly dispersed throughout all the compositions.

- The mechanical test results showed that the tensile strength of 15% Mg composite filaments improved by around 10% compared to the neat PCL filaments, but the elastic modulus decreased by around 50% for the same composition.
- The thermal study revealed that there was a significant reduction in the degradation temperature from above 400°C for pure PCL to around 340°C for PCL/Mg composite having 15% Mg.
- The degradation study showed that the Mg particles enhanced the degradation rate of the PCL matrix.
- Mg incorporation also positively impacted the cell attachment to the PCL/Mg scaffolds with 10wt% Mg.

Overall, incorporating Mg particles into the PCL matrix offers a solution to overcome the low biodegradation typically associated with the PCL and provides enhanced mechanical strength.

5 Future direction

While the current study provides foundational insights into the biocompatibility of our fabricated samples for tissue engineering applications, we recognize the importance of further research to comprehensively assess their potential.

In this context, future studies should include a variety of cell lines, particularly those relevant to specific tissue engineering applications, such as osteoblasts for bone tissue applications, to broaden our understanding of biocompatibility. This would provide a more holistic view of the material's interaction with different cell types. Conducting extended culture periods would be crucial to observe long-term effects, such as chronic toxicity, material degradation over longer durations, and the stability of cell-material interactions over time. This is particularly important for tissue engineering applications where materials are expected to function over extended periods.

To validate *in vitro* findings and assess the clinical potential of the materials, *in vivo* studies using animal models would be an essential next step. These studies would provide critical information on the material's performance in a living system, including its biocompatibility, biodegradation, and integration with host tissues. Ultimately, the goal of tissue engineering research is clinical application. Once sufficient preclinical data is gathered,

conducting clinical trials would be the definitive step in assessing the safety and efficacy of the engineered materials in human patients.

Data availability statement

The raw data supporting the conclusion of this article will be made available by the authors, without undue reservation.

Ethics statement

Ethical approval was not required for the studies on animals in accordance with the local legislation and institutional requirements because only commercially available established cell lines were used.

Author contributions

SN: Conceptualization, Data curation, Investigation, Writing–original draft, Writing–review and editing. FA: Methodology, Supervision, Writing–review and editing, Writing–original draft. KS: Investigation, Methodology, Writing–original draft, Writing–review and editing. OK: Conceptualization, Methodology, Supervision, Writing–review and editing. MP: Investigation, Software, Visualization, Writing–review and editing. CV: Funding acquisition, Resources, Supervision, Writing–review and editing. MK: Funding acquisition, Project administration, Resources, Supervision, Writing–review and editing.

Funding

Acknowledgments

Conflict of interest

The authors declare that the research was conducted in the absence of any commercial or financial relationships that could be construed as a potential conflict of interest.

Publisher's note

All claims expressed in this article are solely those of the authors and do not necessarily represent those of their affiliated organizations, or those of the publisher, the editors and the reviewers. Any product that may be evaluated in this article, or claim that may be made by its manufacturer, is not guaranteed or endorsed by the publisher.

References

Akindoyo, J. O., Beg, M. D. H., Ghazali, S., Heim, H. P., and Feldmann, M. (2017). Effects of surface modification on dispersion, mechanical, thermal and dynamic mechanical properties of injection molded PLA-hydroxyapatite composites. *Compos Part A Appl. Sci. Manuf.* 103, 96–105. doi:10.1016/j.compositesa.2017.09.013

Ali, F., Kalva, S. N., and Koç, M. (2022a). Additive manufacturing of polymer/Mg-based composites for porous tissue scaffolds. *Polym. (Basel)* 14, 5460. doi:10.3390/POLYM14245460

Ali, F., Kalva, S. N., and Koç, M. (2022b). Additive manufacturing of polymer/Mg-based composites for porous tissue scaffolds. *Polym. (Basel)* 14, 5460. doi:10.3390/polym14245460

Ali, F., Kalva, S. N., Mroue, K. H., Keyan, K. S., Tong, Y., Khan, O. M., et al. (2023). Degradation assessment of Mg-Incorporated 3D printed PLA scaffolds for biomedical applications. *Bioprinting* 35, e00302. doi:10.1016/j.bprint.2023.e00302

Antoniac, I., Popescu, D., Zapciu, A., Antoniac, A., Miculescu, F., and Moldovan, H. (2019). Magnesium filled polylactic acid (PLA) material for filament based 3D printing. *Materials* 12, 719. doi:10.3390/ma12050719

Arif, Z. U., Khalid, M. Y., Noroozi, R., Hossain, M., Shi, H. T. H., Tariq, A., et al. (2023). Additive manufacturing of sustainable biomaterials for biomedical applications. *Asian J. Pharm. Sci.* 18, 100812. doi:10.1016/J.AJPS.2023.100812

Arif, Z. U., Khalid, M. Y., Noroozi, R., Sadeghianmaryan, A., Jalalvand, M., and Hossain, M. (2022). Recent advances in 3D-printed polylactide and polycaprolactone-based biomaterials for tissue engineering applications. *Int. J. Biol. Macromol.* 218, 930–968. doi:10.1016/J.IJBIOMAC.2022.07.140

Asadollahi, M., Gerashi, E., Zohrevand, M., Zarei, M., Sayedain, S. S., Alizadeh, R., et al. (2022). Improving mechanical properties and biocompatibility of 3D printed PLA by the addition of PEG and titanium particles, using a novel incorporation method. *Bioprinting* 27, e00228. doi:10.1016/j.bprint.2022.e00228

Bairagi, D., and Mandal, S. (2022). A comprehensive review on biocompatible Mg-based alloys as temporary orthopaedic implants: current status, challenges, and future prospects. *J. Magnesium Alloys* 10, 627–669. doi:10.1016/j.jma.2021.09.005

Bakhshi, R., Mohammadi-Zerankeshi, M., Mehrabi-Dehdezi, M., Alizadeh, R., Labbaf, S., and Abachi, P. (2023a). Additive manufacturing of PLA-Mg composite scaffolds for hard tissue engineering applications. *J. Mech. Behav. Biomed. Mater* 138, 105655. doi:10.1016/J.JMBBM.2023.105655

Bakhshi, R., Mohammadi-Zerankeshi, M., Mehrabi-Dehdezi, M., Alizadeh, R., Labbaf, S., and Abachi, P. (2023b). Additive manufacturing of PLA-Mg composite scaffolds for hard tissue engineering applications. *J. Mech. Behav. Biomed. Mater* 138, 105655. doi:10.1016/j.jmbbm.2023.105655

Chen, K.-J., Hung, F.-Y., Wang, Y.-T., and Yen, C.-W. (2022). Mechanical properties and biomedical application characteristics of degradable polylactic acid–Mg–Ca3(PO4)2 three-phase composite. *J. Mech. Behav. Biomed. Mater* 125, 104949. doi:10.1016/j.jmbbm.2021.104949

Cheng, C. H., Shie, M. Y., Lai, Y. H., Foo, N. P., Lee, M. J., and Yao, C. H. (2021). Fabrication of 3D printed poly(lactic acid)/polycaprolactone scaffolds using TGF-β1 for promoting bone regeneration. *Polym. (Basel)* 13, 3731. doi:10.3390/POLYM13213731

Dong, Q., Zhang, M., Zhou, X., Shao, Y., Li, J., Wang, L., et al. (2021). 3D-printed Mg-incorporated PCL-based scaffolds: a promising approach for bone healing. *Mater. Sci. Eng. C* 129, 112372. doi:10.1016/j.msec.2021.112372

Dwivedi, R., Kumar, S., Pandey, R., Mahajan, A., Nandana, D., Katti, D. S., et al. (2020). Polycaprolactone as biomaterial for bone scaffolds: review of literature. *J. Oral Biol. Craniofac. Res.* 10, 381–388. doi:10.1016/J.JOBCR.2019.10.003

Ferrández-Montero, A., Lieblich, M., Benavente, R., González-Carrasco, J. L., and Ferrari, B. (2020). Study of the matrix-filler interface in PLA/Mg composites manufactured by Material Extrusion using a colloidal feedstock. *Addit. Manuf.* 33, 101142. doi:10.1016/j.addma.2020.101142

Galow, A. M., Rebl, A., Koczan, D., Bonk, S. M., Baumann, W., and Gimsa, J. (2017). Increased osteoblast viability at alkaline pH *in vitro* provides a new perspective on bone regeneration. *Biochem. Biophys. Rep.* 10, 17–25. doi:10.1016/J.BBREP.2017.02.001

Gollwitzer, H., Thomas, P., Diehl, P., Steinhauser, E., Summer, B., Barnstorf, S., et al. (2005). Biomechanical and allergological characteristics of a biodegradable poly(D,L-lactic acid) coating for orthopaedic implants. *J. Orthop. Res.* 23, 802–809. doi:10.1016/j.orthres.2005.02.003

Hasanpur, E., Ghazavizadeh, A., Sadeghi, A., and Haboussi, M. (2021). *In vitro* corrosion study of PLA/Mg composites for cardiovascular stent applications. *J. Mech. Behav. Biomed. Mater* 124, 104768. doi:10.1016/j.jmbbm.2021.104768

Kalva, S. N., Ali, F., Velasquez, C. A., and Koç, M. (2023). 3D-Printable PLA/Mg composite filaments for potential bone tissue engineering applications. *Polymers* 15, 2572. doi:10.3390/POLYM15112572

Khoo, L. K., Kiattavorncharoen, S., Pairuchvej, V., Lakkhanachatpan, N., Wongsirichat, N., and Seriwatanachai, D. (2020). The affinity of human fetal osteoblast to laser-modified titanium implant fixtures. *Open Dent. J.* 14, 52–58. doi:10.2174/1874210602014010052

Leonés, A., Salaris, V., Ramos Aranda, I., Lieblich, M., López, D., and Peponi, L. (2023). Thermal properties and *in vitro* biodegradation of PLA-Mg filaments for fused deposition modeling. *Polymers* 15, 1907. doi:10.3390/POLYM15081907

Liang, J.-Z., Duan, D.-R., Tang, C.-Y., Tsui, C.-P., and Chen, D.-Z. (2013). Tensile properties of PLLA/PCL composites filled with nanometer calcium carbonate. *Polym. Test.* 32, 617–621. doi:10.1016/j.polymertesting.2013.02.008

Malikmammadov, E., Tanir, T. E., Kiziltay, A., Hasirci, V., and Hasirci, N. (2018). PCL and PCL-based materials in biomedical applications. *J. Biomater. Sci. Polym.* 29, 863–893. doi:10.1080/09205063.2017.1394711

Muley, S. V., Vidvans, A. N., Chaudhari, G. P., and Udainiya, S. (2016). An assessment of ultra fine grained 316L stainless steel for implant applications. *Acta Biomater.* 30, 408–419. doi:10.1016/j.actbio.2015.10.043

Noroozi, R., Arif, Z. U., Taghvaei, H., Khalid, M. Y., Sahbafar, H., Hadi, A., et al. (2023). 3D and 4D bioprinting technologies: a game changer for the biomedical sector? *Ann. Biomed. Eng.* 51 (8 51), 1683–1712. doi:10.1007/S10439-023-03243-9

Razavi, M., and Huang, Y. (2019). Assessment of magnesium-based biomaterials: from bench to clinic. *Biomater. Sci.* 7, 2241–2263. doi:10.1039/c9bm00289h

Shayesteh Moghaddam, N., Taheri Andani, M., Amerinatanzi, A., Haberland, C., Huff, S., Miller, M., et al. (2016). Metals for bone implants: safety, design, and efficacy. *Biomanufacturing Rev.* 1, 1. doi:10.1007/s40898-016-0001-2

Shuai, C., Li, Y., Feng, P., Guo, W., Yang, W., and Peng, S. (2018). Positive feedback effects of Mg on the hydrolysis of poly-l-lactic acid (PLLA): promoted degradation of PLLA scaffolds. *Polym. Test.* 68, 27–33. doi:10.1016/j.polymertesting.2018.03.042

Singh, D., Singh, R., Boparai, K. S., Farina, I., Feo, L., and Verma, A. K. (2018). *In-vitro* studies of SS 316 L biomedical implants prepared by FDM, vapor smoothing and investment casting. *Compos B Eng.* 132, 107–114. doi:10.1016/j.compositesb.2017.08.019

Song, G. L., and Atrens, A. (1999). Corrosion mechanisms of magnesium alloys. *Adv. Eng. Mater* 1, 11–33. doi:10.1002/(SICI)1527-2648(199909)1:1<11::AID-ADEM11>3.0.CO;2-N

Tran, H. N., Kim, I. G., Kim, J. H., Chung, E. J., and Noh, I. (2022). Control of maleic acid-propylene diepoxide hydrogel for 3D printing application for flexible tissue engineering scaffold with high resolution by end capping and graft polymerization. *Biomater. Res.* 26, 75–19. doi:10.1186/s40824-022-00318-x

Tsakiris, V., Tardei, C., and Clicinschi, F. M. (2021). Biodegradable Mg alloys for orthopedic implants – a review. *J. Magnesium Alloys* 9, 1884–1905. doi:10.1016/j.jma.2021.06.024

Tzeng, J.-J., Hsiao, Y.-T., Wu, Y.-C., Chen, H., Lee, S.-Y., and Lin, Y.-M. (2018). Synthesis, characterization, and visible light curing capacity of polycaprolactone acrylate. *Biomed. Res. Int.* 2018, 1–8. doi:10.1155/2018/8719624

Wang, F., Tankus, E. B., Santarella, F., Rohr, N., Sharma, N., Märtin, S., et al. (2022). Fabrication and characterization of PCL/HA filament as a 3D printing material using thermal extrusion technology for bone tissue engineering. *Polym. (Basel)* 14, 669. doi:10.3390/polym14040669

Xiang, D. D., Wang, P., Tan, X. P., Chandra, S., Wang, C., Nai, M. L. S., et al. (2019). Anisotropic microstructure and mechanical properties of additively manufactured Co–Cr–Mo alloy using selective electron beam melting for orthopedic implants. *Mater. Sci. Eng. A* 765, 138270. doi:10.1016/j.msea.2019.138270